van der Waals Interactions in Density Functional Theory Using Wannier Functions

Pier Luigi Silvestrelli*

Dipartimento di Fisica "G. Galilei", Università di Padova, via Marzolo 8, I-35131 Padova, Italy, and DEMOCRITOS National Simulation Center, Trieste, Italy

Received: December 17, 2008; Revised Manuscript Received: March 6, 2009

van der Waals interactions between atoms and molecules are ubiquitous and very important for many molecular and condensed-matter structures. These systems are often studied from first principles using the density functional theory (DFT), because this approach often represents a good compromise between accuracy and efficiency. However, the commonly used DFT functionals are not able to describe properly van der Waals effects. Most attempts to correct for this problem have a basic semiempirical character, although computationally more expensive first principles schemes have been recently developed. Of course, the key issue is finding a way to include van der Waals interactions in DFT without dramatically increasing the computational cost. We here describe in detail the recently developed scheme, based on the use of the maximally localized Wannier functions, that combines the simplicity of the semiempirical formalism with the accuracy of the first principles approaches and appears to be promising, being simple, efficient, accurate, and transferable (for instance, charge polarization effects are naturally included). The results of successful applications to small molecules, bulk Ar, and the interaction of Ar, He, and H_2 with two different Al surfaces are presented. Directions for further improvements of the method are finally suggested.

I. Introduction

Density functional theory (DFT) represents an efficient and popular tool to study the structural and electronic properties of molecules and condensed matter systems from first principles and to elucidate complex processes such as surface adsorptions, catalytic reactions, and diffusive motions. Although current density functionals are able to describe well several systems, at much lower computational cost compared to other first principles methods, they fail to do so[1] for the description of long-range dispersion effects, generally denoted as van der Waals (VdW) interactions, particularly the leading R^{-6} term due to correlated instantaneous dipole fluctuations; some cases where DFT (using, for instance, the Perdue−Burke−Ernzerhof (PBE) functional[2]) provides reasonable estimates for the interaction energy of weakly bound systems are actually due to favorable errors or cancelations and should therefore be considered accidental.

To overcome this severe deficiency of DFT, two basic strategies have been adopted: on one hand, new density functionals or/and relatively complex schemes have been proposed that allow for a first-principles treatment of the VdW interactions;[1,3−8] on the other hand several semiempirical approaches[9−13] have been developed where an approximately derived R^{-6} term, multiplied by a suitable short-range damping function, is explicitly introduced. Although both these approaches have been somehow successful, neither of them appears to be entirely satisfactory: in fact, the former is generally quite complex and computationally demanding, compared to a standard DFT calculation, while the latter, based on interatomic C_6 coefficients (that would actually be dependent on the molecular environment of the atoms involved) and empirical fits, turns out to be far from generally applicable because it neglects changes in the atomic polarizabilities (which, in general, are not additive) and should be tailored to the specific system considered. Therefore the development of a practical efficient scheme to include VdW interactions in DFT still represents an important goal. Of course, the crucial issue is to include dispersion forces in DFT without dramatically increasing the computational cost.

In this paper we present a detailed description, with some improvements and extensions, of a method we have recently introduced in a published letter,[14] which allows the efficient calculation of the VdW interactions between nonoverlapping fragments, using as input only the ground-state electron density and the Kohn−Sham (KS) orbitals computed in a conventional DFT approach.

II. Methods

Typical fragment−fragment interactions can be separated into short-range interactions, which depend explicitly on the overlapping of the electron densities and vanish at distances that are sufficiently large that this overlap becomes negligible, and long-range, dispersive interactions, with a leading term varying as the inverse 6th power of the fragment−fragment distance.

The idea of using a localized description for electron correlation goes back to 40 years, and many different local correlation methods have been proposed since then.[15] For instance, in insulators, the occupied Hartree−Fock (HF) manifold can be represented as an antisymmetrized product of well localized Wannier functions, and a periodic local correlation scheme for the solution of MP2 equations has been developed.[15]

In our method we use the maximally localized Wannier function (MLWF) formalism[16] that allows the total electronic density to be partitioned, in a chemically transparent and unambiguous way, into individual fragment contributions.[17] The MLWFs represent a generalization, for systems characterized by periodic boundary conditions, of the Boys' localized orbitals[18] that are commonly used in quantum chemistry; they allow for an intuitive interpretation of the bonding properties of condensed-

* To whom correspondence should be addressed. E-mail: psil@pd.infn.it.

10.1021/jp811138n CCC: $40.75
Published on Web 04/03/2009

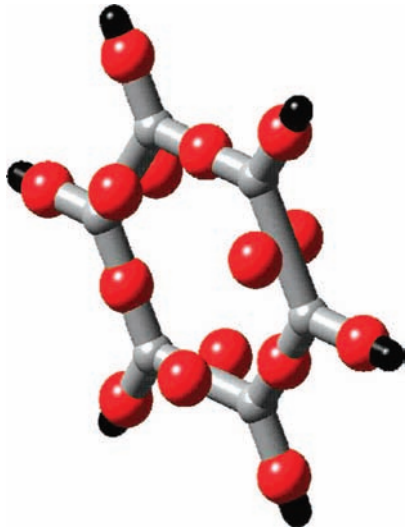

Figure 1. Distribution of the WFCs, denoted by the balls, in the case of the benzene molecule.

matter systems[16] and are at the center of the modern theory of polarization.[19]

The MLWFs, $\{w_n(r)\}$, are generated by performing a unitary transformation in the subspace of the occupied KS orbitals, obtained by a standard DFT calculation, so as to minimize the functional Ω, defined as

$$\Omega = \sum_n S_n^2 = \sum_n (\langle w_n|r^2|w_n\rangle - \langle w_n|\mathbf{r}|w_n\rangle^2) \tag{1}$$

The measure of the localization (the spread functional) is a global property of the MLWF set as a whole; this means that even if we are reaching lower and lower values of the spread, the set of MLWFs we found is a "good one" only if each individual MLWF is localized (in fact a single, not properly localized, WF could make the whole set useless). Reasonable criteria, derived from a large number of applications and test experiences, are the following:[20] typically the spread of each WF should be not larger than about 2.5 Å, and the spatial decay of the Hamiltonian $\hat{H}(R)$ on the MLWF basis is expected to be nearly exponential as a function of R.

Besides its spread, S_n, each MLWF is characterized also by its Wannier function center (WFC); for instance, if periodic boundary conditions are used with a cubic supercell of side L, the coordinate x_n of the nth WFC is defined[16] as

$$x_n = -\frac{L}{2\pi} Im \ln\langle w_n|e^{-i\frac{2\pi}{L}x}|w_n\rangle \tag{2}$$

with similar definitions for y_n and z_n. If spin degeneracy is exploited, every MLWF corresponds to 2 paired electrons. Suitable codes[20] are available, which allow the efficient generation of the MLWFs, even by adopting a proper k-point sampling of the Brillouin Zone (BZ), which is crucial, for instance, in metallic systems. In Figure 1 we show the distribution of the WFCs in the case of the benzene molecule: the 30 valence electrons are described by 15 MLWFs (due to spin degeneracy).

Starting from these MLWFs the leading R^{-6} VdW correction term can be evaluated using different possible recipes; one of them is described and applied in the following. We make the reasonable assumption[21] of exponential localization of the MLWFs in real space, so that each of them is supposed to be an hydrogenlike, normalized, function, centered around its WFC position, r_n, with a spread S_n

$$w_n(|\mathbf{r}-\mathbf{r}_n|) = \frac{3^{3/4}}{\sqrt{\pi}S_n^{3/2}} e^{-\frac{\sqrt{3}}{S_n}|\mathbf{r}-\mathbf{r}_n|} \tag{3}$$

Our assumption is also supported by the fact that the molecular orbitals often resemble the wave functions of a free electron in a cavity of the same size as that of the volume occupied by the selected molecule.[22]

Given the MLWFs, the binding energy of a system composed of two fragments can be obtained as $E_b = E_0 + E_{VdW}$, where E_0 is the binding energy computed with a standard DFT calculation, while the VdW correction is assumed to have the form

$$E_{VdW} = -\sum_{n,l} f_{nl}(r_{nl}) \frac{C_{6nl}}{r_{nl}^6} \tag{4}$$

where r_{nl} is the distance of the n-th WFC, of the first fragment, from the l-th WFC of the second one, the sum is over all the MLFWs of the two fragments, and the C_{6nl} coefficients can be calculated directly from the basic information (center positions and spreads) given by the MLFWs. In fact, using for instance the expression proposed by Andersson, Langreth, and Lundqvist (see eq 10 of ref 4), hereafter referred as the ALL functional, that describes the long-range interaction between two separated fragments of matter

$$C_{6nl} = \frac{3}{32\pi^{3/2}} \int_{|\mathbf{r}|\le r_c} d\mathbf{r} \int_{|\mathbf{r}'|\le r_c'} d\mathbf{r}' \frac{\sqrt{\rho_n(r)\rho_l(r')}}{\sqrt{\rho_n(r)} + \sqrt{\rho_l(r')}}$$

$$= \frac{3}{32\pi^{3/2}} \int_{|\mathbf{r}|\le r_c} d\mathbf{r} \int_{|\mathbf{r}'|\le r_c'} d\mathbf{r}' \frac{|w_n(r)||w_l(r')|}{|w_n(r)| + |w_l(r')|} \tag{5}$$

where $\rho_n(r) = w_n^2(r)$ is the electronic density corresponding to the nth MLWF, C_{6nl} is given in au, and the r_c, r_c' cutoffs have been introduced[3,4] to properly take into account both the limit of separated fragments and of distant disturbances in an electron gas; by equating the length scale for density change to the electron gas screening length one obtains

$$\frac{6\rho_n(r_c)}{|\vec{\nabla}\rho_n(r_c)|} = \frac{v_F[\rho_n(r_c)]}{\omega_p[\rho_n(r_c)]} \tag{6}$$

where $v_F = (3\pi^2\rho_n(r))^{1/3}/m$ is the local Fermi velocity, and $\omega_p = (4\pi e^2\rho_n(r)/m)^{1/2}$ is the local plasma frequency. By use of the analytic form (see eq 3) of the MLWFs, it is straightforward to obtain the cutoff expressed in terms of the MLWF spread

$$r_c = S_n\sqrt{3}(0.769 + 1/2\ln(S_n)) \tag{7}$$

and to evaluate very efficiently the multidimensional integral of eq 5

$$C_{6nl} = \frac{S_n^{3/2}S_l^3}{2 \cdot 3^{5/4}} F(S_n, S_l) \tag{8}$$

where

$$F(S_n, S_l) = \int_0^{x_c} dx x^2 e^{-x} \int_0^{y_c} dy \frac{y^2 e^{-y}}{e^{-x}/\beta + e^{-y}} \tag{9}$$

and

$$\beta = \frac{S_n^{3/2}}{S_l} \qquad x_c = \sqrt{3}r_c/S_n \qquad y_c = \sqrt{3}r_c'/S_l \tag{10}$$

For instance, in the test case of two, distant H atoms, using the well-known (unperturbed) analytic H atom wave function,

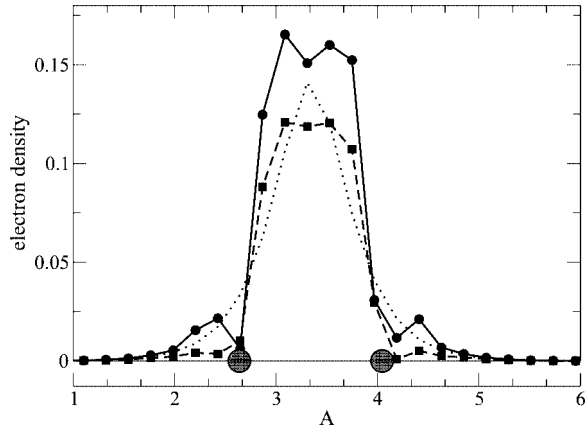

Figure 2. Electron density profile (in Bohr^{-3}) plotted along an axis containing a pair of nearest-neighbor C atoms of the benzene molecule: the solid line (with circles) denotes the contribution obtained when a "single"-bond MLWF is considered (corresponding, in Figure 1, to the cases where there is only one WFC between the two C atoms), while the dashed line (with squares) denotes the contribution obtained when two "double"-bond MLWFs are considered (corresponding, in Figure 1, to the cases where there are two WFCs between the two C atoms); in the latter case, the dotted curve shows the density obtained by replacing the two actual MLWFs by their H-like approximants (see eq 3). The two large gray balls indicate the positions of the C atoms.

one has that $S = \sqrt{3}$ au, so that the above formula gives $C_6 = 6.41$ au to be compared to the reference literature value of 6.50 au.[23]

In eq 5, if the electronic density corresponding to every MLWF is multipled by 2, the C_{6nl} coefficients increase by a factor of $\sqrt{2}$; therefore it appears reasonable to assume that, when each MLWF describes 2 paired electrons (spin degeneracy), C_{6nl} has to be multipled by $\sqrt{2}$. This is also supported by the fact that in the Slater−Kirkwood approximation for estimating the C_6 coefficients the effective number of electrons is smaller than the number of valence electrons, and it is $1.42 \simeq \sqrt{2}$ in the case of the He atom,[24] whose DFT ground state is just given by 2 paired electrons in the lowest-energy KS orbital.

Figure 2 shows the electron density profile, for the benzene molecule, plotted along the C−C bond and compared to the same quantity obtained from the H-like function approximants, which are supposed to mimic the actual MLWFs: we consider the two different cases (see Figure 1), namely, the "double" C−C bond (described by two MLWFs) and the "single" C−C bond (described by a single MLWF). As can be seen, the H-like approximation appears to be reasonable, particularly if one considers that it is the spread of the localized functions rather than its detailed shape which mostly matters in the present scheme based on the local-polarizability approximation; moreover the profiles relative to the two different cases are not very different, in spite of the evident symmetry-breaking induced by the MLWF generation; of course this is not unexpected since the C−C nearest-neighbor distances in the optimized structure of the benzene molecule are identical. The 6-fold rotational-symmetry breaking (bonding orbitals between different C−C pairs differ) and the lack of symmetry in the chemical picture of benzene, as obtained by generating the MLWFs from the occupied KS orbitals, is a result of ignoring the 3 antibonding π orbitals of the C ring in the construction of the MLWFs; including these 3 extra states restores the 6-fold rotational symmetry.[25]

In eq 4, $f_{nl}(r)$ is a damping function which serves to cutoff the unreasonable behavior of the asymptotic VdW correction at small fragment separations. For it we have chosen a form[12,26] with parameters directly related to the MLWF spreads

$$f_{nl}(r) = \frac{1}{1 + \exp(-a(r/R_s - 1))} \tag{11}$$

where[26] $a \simeq 20$ (the results are almost independent of the particular value of this parameter) and $R_s = R_{VdW} + R'_{VdW}$ is the sum of the VdW radii of the MLWFs. In our first paper[14] R_{VdW} was determined as the radius of the 0.01 Bohr^{-3} electron density contour. For general applications, including also extended systems with metal or semimetal surfaces, after extensive testing, we found that a better choice is to equate R_{VdW} to the cutoff radius introduced in eqs 5−7, $R_{VdW} = r_c$, which has the additional advantage of not being dependent on any given electron density threshold. It should be stressed that the results reported in ref 14, relative to isolated fragments and bulk graphite, are essentially unchanged if recomputed by adopting this new R_{VdW} definition. The effect of using different damping functions is described, for selected applications, in the result section.

The damping function effectively reduces the VdW correction to zero at short distances; at intermediate distances a minimum in the VdW potential exists that usually lies around the sum of the corresponding VdW radii, R_s. The need of using suitable damping functions implies a certain amount of arbitrariness and reflects the fundamental difficulty of an unambiguous separation between short-range interactions (where $a\ -C_6/R^6$ behavior is clearly unphysical) and long-range ones (where $a\ -C_6/R^6$ behavior is valid), particularly in the DFT exchange-correlation contribution. Note that the above recipe resembles that proposed in ref 27, where the long-range electron−electron interaction is separated from the short-range one, using a single parameter describing the physical dimensions of a valence electron pair.

The overlap between different MLWFs can be qualitatively assessed by comparing the sum of their spreads to the distance between their centers; clearly, the overlap is small whenever the former is much smaller than the latter. One must also distinguish between the overlap between MLWFs belonging to the same fragment (intrafragment) and between MLWFs belonging to different fragments (interfragment), which is much more relevant for the present scheme, where we compute an interfragment VdW correction. For instance, in the case of water molecules in the liquid phase, the typical MLWF spread is found to be[28] ∼0.7 Å, much smaller than the intermolecular distances (the O−O nearest-neighbor distance is about 2.8 Å in liquid water), and the MLWF charge overlap is estimated[28] to be 0.2 for different MLWFs of the same water molecule, while it is smaller than 0.01 for MLWFs located on different molecules. The same is true also in the case of the benzene dimer considered in the present study, in fact the MLWF spreads are within the range 0.7−1.1 Å, so that the cutoff defined in eq 6 is within the range 0.7−1.5 Å, while the characteristic equilibrium distances are larger than 3.7 Å. In general, also taking the contribution of the damping function into account, which suppresses the short-range corrections, one expects that the effect of the MLWF interfragment overlap is negligible, except for metallic systems where it could be of importance. The intrafragment overlap is of course larger, however, in the spirit of the ALL formalism,[4] where a local-polarizability approximation is adopted so that the contribution from the tails of the wave functions (where the length scale for the density change is much shorter than the electron gas screening length) is neglected, its effect is expected to be much less important.

The E_0 binding energy can be obtained from a standard DFT calculation (we have used both the CPMD[29] and the Quantum-ESPRESSO[30] ab initio packages), using the generalized gradient approximation (GGA), typically in the revPBE flavor.[31] This

choice[8,26] is motivated by the fact that revPBE is fitted to the exact HF exchange, so that it usually gives results close to those obtained by HF, and the VdW binding, a correlation effect, only comes from the VdW correction term, as described above, without any double-counting effect (for instance, the local density approximation or some GGA functionals, such as PBE, predict substantial binding in rare gas dimers, due to a severe overestimate of the long-range part of the exchange contribution[8]). The evaluation of the VdW correction as a poststandard DFT perturbation, using the revPBE electronic density distribution, represents an approximation because in principle full self-consistent calculations should be performed; however recent investigations[32] on different systems have shown that the effects due to the lack of self-consistency are negligible (this is reasonable because one does not expect that the rather weak and diffuse VdW interaction substantially changes the electronic charge distribution). In any case, in principle, the implementation of a self-consistent version of the method would be not more difficult than for other first-principles schemes where DFT is corrected by VdW effects.

The present method has some similarities with the LC-DFT + ALL approach proposed and successfully applied to describe weak interactions between small molecules by Sato et al.,[33] who developed a long-range correction to GGA functionals, based on the same ALL functional of eq 5 and adopting a suitable damping functions. In both the methods the VdW correction is evaluated by considering the interaction between localized electron-charge density distributions, belonging to separate fragments. The main difference between the two schemes is given by the fact that while in the LC-DFT + ALL method the localized electron density is that of the atoms which constitute the fragments in the present one is that of the MLWFs. A VdW correction scheme based on atomic densities has also been very recently proposed by Tkatchenko and Scheffler.[34]

The VdW correction scheme described above can be refined by considering the effects due to the anisotropy of the MLWFs and distinguishing between contributions along (or orthogonal to) the fragment−fragment direction,[14] as described in detail in Appendix A.

When periodic systems are considered, it is necessary to modify our algorithm in such a way to include interactions of the MLWFs of the selected fragment (i.e., a physisorbed molecule or a single atom in a bulk crystal) not only with the other MLWFs, within the reference supercell, but also with a sufficient number of periodically repeated MLWFs (in any case, given the R^{-6} decay of the VdW interactions the convergence is rapidly achieved).

In principle, also higher-order term VdW corrections, involving the C_8, C_{10},... coefficients, could be included following a similar derivation scheme (C_8/R^8 terms are expected to contribute to the dispersion energy for an amount of the order of $^1/_3$ of the dominant C_6/R^6 terms[35]).

Clearly, in the present method, the evaluation of the VdW corrections to the interfragment forces is trivial, thus allowing an easy implementation in standard geometry optimization calculations or molecular dynamics simulations (see Appendix B).

Remarkably, the whole procedure of generating the MLWFs and evaluating the VdW corrections represents a negligible additional computational cost, compared to that of a standard DFT calculation. In fact the evolution toward the minimum of the functional Ω (see eq 1) requires only the relatively inexpensive updating of unitary matrices and not of the wave functions themselves.[16] This makes the calculation of the Wannier functions very efficient. Actually the goal of a linear scaling of electronic structure calculations, based on localized (in space) orbitals, was at the heart of the motivation for the original work of Marzari and Vanderbilt.[16] At present, very efficient algorithms for obtaining MLWFs exist (see for instance Berghold et al.,[36] and Iannuzzi and Parrinello[37]); moreover MLWFs can be also generated within a Car−Parrinello molecular dynamics approach (thus allowing to follow the trajectories of the MLWFs) with only a modest increase in computational time: for instance, the additional cost is about 10% for a system made of 64 water molecules (Thomas et al.,[38] Iftimie et al.,[39] Souza et al.[40]). In fact the computational overhead of the rotation step required to generate the MLWFs is roughly equal to the cost of a Car−Parrinello step, which corresponds to a single step in the procedure of converging the wave functions in a standard plane-wave based ab initio code. Therefore the cost of the localization procedure scales linearly with the number of electrons in the system.[39]

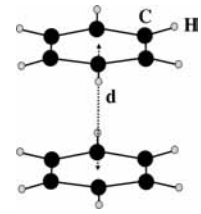

Figure 3. Benzene dimer in the S configuration.

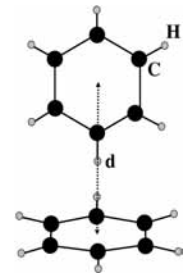

Figure 4. Benzene dimer in the T configuration.

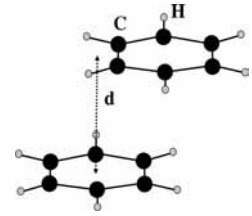

Figure 5. Benzene dimer in the PD configuration.

In our calculations, the wave functions were expanded in plane waves, with an energy cutoff of 50 Ry for the benzene dimer and the SiH_4−CH_4 complex and of 70 Ry for the other systems investigated. Suitable norm-conserving pseudopotentials have been adopted; in this scheme, the use of a pseudopotential approach is justified because only the most loosely bound electrons essentially contribute to the polarizability.[41]

III. Results

A. Benzene Dimer. A very sensitive test for the quality of the dispersion corrections is represented by the benzene dimer. The basic configurations of this system (see Figures 3, 4, and 5) are the sandwich (S), the T-shaped (T), and the parallel-displaced (PD) conformations. The substantial attractive interaction in benzene dimer, even when the molecules are well separated, shows that the major source of attraction is not short-

range (the energies of short-range interactions, which arise where the molecular wave functions overlap significantly, decrease exponentially with distance) such as charge-transfer but long-range interactions (where the energy of interaction behaves as some inverse power of the distance) such as dispersion and electrostatic. Dispersion is only one of the main forces determining the potential surface of the benzene dimer; electrostatic (quadrupole−quadrupole) interaction, which is highly orientation dependent, is also important, as it is shown by the fact that the T-shaped conformer, that has favorable electrostatics but weaker dispersion, in high-quality quantum chemistry calculations (HQ) is close in energy to the PD configuration that has more dispersion but less favorable electrostatic. Pauli repulsion, together with repulsive quadrupole−quadrupole forces, is probably responsible for the energy maximum in the S conformation (see Figure 3); the S geometry represents a saddle point on the potential energy surface and is much less strongly bound than either of the other two principal forms and is thus the least significant as a candidate for $\pi-\pi$ interactions in biological systems. Although the favored structures are undoubtedly the T and PD, which one is the lowest-energy configuration is still controversial: in fact the T-shaped structure is clearly preferred by HF and standard DFT methods because it has larger (attractive) electrostatic interactions than the PD form, which is instead more stabilized by dispersion;[42] however, local density approximation (LDA) favors the PD geometry, and only the T form is bound at the pure PBE level. In any case, DFT-GGA functionals turn out to be unsuitable[43] for the description of benzene dimers, and except for unreasonable distances, the dimers fail to bond. Even using HQ calculations, in the literature there is no consensus about the minimum-energy configuration: according to Janowski and Pulay,[44] the T-shaped geometry is marginally (by about 0.02 kcal/mol) more stable than the PD one at all levels of the theory after counterpoise correction, except at the lowest (DZ) level; MP2, by contrast, predicts the PD displaced form to be more stable by about 1 kcal/mol (∼43 meV); the reason for this is probably the overestimation of the dispersive $\pi-\pi$ interactions by MP2.[45]

Another difficulty is due to the fact that interactions between benzene dimers are clearly highly anisotropic, mainly because of the presence of $\pi-\pi$ interactions (see also Figure 1). The importance of this kind of interactions has been stressed repeatedly in many fields of chemistry from molecular biology to material design. The $\pi-\pi$ interaction influences the 3D structures of biological systems such as protein and DNA and is crucial for the crystal packing of organic molecules containing aromatic rings such as nonlinear optical materials; this is also relevant for molecular recognition processes in biological and artificial systems.[45] The simplest theory of dispersion predicts that it is proportional to the product of the polarizabilities of the two subsystems, and therefore it is particularly strong for groups with high polarizability like π systems.

There are two experimental estimates for the binding energy (where geometry was not modeled) of the benzene dimer: 1.6 ± 0.2 kcal/mol = 69 ± 9 meV[46] and 2.4 ± 0.4 kcal/mol = 104 ± 17 meV;[47] on the basis of high-quality calculations, the higher value is probably the most reliable one.[44] Experimental measurements of the benzene T dimer center-of-mass separation found a distance of 4.96 Å.[48]

For simulating this system (and also the other small molecules investigated in this study) we have chosen a simple cubic supercell, with a side of 30 au (thus making the interactions among periodic replicas of the molecules negligible) and a sampling of the BZ limited to the Γ point; even the benzene monomer geometry was fully relaxed during dimer structure optimization, although it changes very little in the dimer.[49] For this complex the characteristic distance, d, is given (see Figures 3−5) by the center of mass-separation for the S and T structures, and the distance between the molecular planes for the PD configuration (in this case the optimal lateral shift of the molecules was found to be 1.64 Å). In comparing equilibrium distances with reference values, one should keep in mind that the potential energy surfaces associated with weak binding are much flatter than those associated with, for example, covalent bonding, so that errors in determining the optimal monomer separations of the order of 0.1 Å are to be expected.

In Tables 1 and 2 we report our results compared to those obtained using other methods and with the available experimental estimates. As can be seen, the improvement obtained by adding the VdW corrections to the pure revPBE description (in which only the T configuration is slightly bonded) is dramatic, and the results are compatible with the experimental data, although the agreement with high-quality calculations is not perfect: in fact we predict that the PD structure is the favored

TABLE 1: Binding Energy, in kcal/mol, of Different Configurations (S, PD, T) of the Benzene Dimer (Figures 3−5) Computed Using the Standard revPBE Calculation and Adding the VdW Correction[a]

method	S	PD	T
LDA	−1.04	−2.70	−2.19
LC-DFT + ALL	−1.89	−2.56	−2.75
GGA + SEMI	−4.59 ↔ −1.78	−5.99 ↔ −2.74	−6.39 ↔ −2.61
HQ	−1.80 ↔ −1.48	−2.79 ↔ −2.49	−2.74 ↔ −2.47
revPBE			−0.30
revPBE + VdW	−1.94 (−1.80)	−2.26 (−2.28)	−1.94 (−1.87)
PBE + VdW	−2.58	−3.83	−3.09
BLYP + VdW	−1.52	−1.94	−1.64

[a] In parentheses, values computed taking anisotropy effects into account are reported. The values are compared to those obtained by adding the VdW correction to standard PBE and BLYP calculations, to the LDA estimate,[11] to values obtained by the LC-DFT + ALL method of Sato et al.,[33] and to other GGA + VdW semiempirical correction schemes (GGA + SEMI) reported in the literature[11,70,71] and by high-quality, quantum chemistry (HQ) calculations.[44,45,49,70] The experimental estimates for the binding energy (where geometry was not precisely characterized) are −1.6 ± 0.2 kcal/mol[46] and 2.4 ± 0.4 kcal/mol.[47]

TABLE 2: Equilibrium Characteristic Distance (See Text and Figures 3−5 for Definitions), d, in Å, of Different Configurations (S, PD, T) of the Benzene Dimer, Computed Using the Standard revPBE Calculation, and Adding the VdW Correction[a]

method	S	PD	T
LDA	3.78	3.32	4.77
LC-DFT + ALL	4.10	3.60	5.00
GGA + SEMI	3.70 ↔ 3.90	3.36 ↔ 3.51	4.82 ↔ 5.00
HQ	3.89 ↔ 3.92	3.53 ↔ 3.55	4.99 ↔ 5.04
revPBE			5.83
revPBE + VdW	4.39 (4.34)	3.97 (3.76)	5.32 (5.48)
PBE + VdW	4.00	3.67	4.94
BLYP + VdW	4.16	4.10	5.14

[a] In parentheses, values computed taking anisotropy effects into account are reported. The values are compared to those obtained by adding the VdW correction to standard PBE and BLYP calculations, to the LDA estimate,[11] to values obtained by the LC-DFT + ALL method of Sato et al.,[33] and other GGA + VdW semiempirical correction schemes (GGA + SEMI) reported in the literature[11,70,71] and by high-quality, quantum chemistry (HQ) calculations.[44,45,49,70] The experimental estimate[48] of the interdimer distance, in the T configuration, is 4.96 Å.

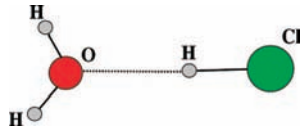

Figure 6. H_2O-HCl molecule.

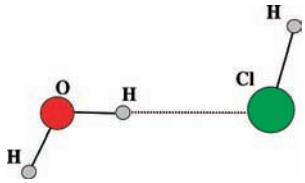

Figure 7. HOH-ClH molecule.

one, while the S and T are essentially isoenergetic. Moreover the equilibrium distances appear to be overestimated, a behavior probably related to our use of the revPBE functional, as suggested also in refs.[8,32] The results are only slightly changed by taking the anisotropy of the MLWFs into account. We also report the corresponding values obtained by using PBE or BLYP as the reference DFT functional instead of revPBE; as expected, the BLYP functional gives results similar to revPBE. With PBE+VdW and BLYP+VdW the S configuration is less favored with respect to the T and PD, than using revPBE+VdW, which is more in line with the expected behavior. Moreover, PBE+VdW reproduces well the experimental estimate of the interdimer distance of the T configuration, namely 4.96 Å. Interestingly, this is another case in which LDA performs better than pure GGA, while the binding energies given by different GGA+VdW semiempirical correction schemes are largely scattered. Note that, using the "seamless" method of Langreth et al., the only literature reported values (binding energy of about −2.3 kcal/mol and equilibrium distance of about 4.1Å) are relative to the S configuration,[8] and are not far from ours. As can be seen in Tables 1 and 2, the binding energies and the equilibrium intermolecular distances of the benzene dimers are well reproduced by the LC-DFT+ALL method of Sato et al.,[33] who obtained results in agreement with HQ calculations.

B. H_2O-HCl and HOH-ClH. When the HCl molecule interacts with a water molecule, the favored structure is represented by the H_2O-HCl complex (see Figure 6), where an H-bond is formed between O and HCl, so that HCl elongates slightly, while the geometry of water is not significantly different from that of the isolated molecule. However, another, much more weakly bonded configuration, namely, HOH-ClH (Figure 7), characterized by a very weak H-bond between Cl and OH, could be of interest, for instance, to rationalize the formation of interfacial water on the Cl-terminated Si(111) surface.[50] Interestingly, in this latter case, the contribution of dispersive interactions is much more important, due to the weakness of the H bond.

In the Tables 3 and 4 we report our results compared to those obtained using other methods (HF and MP2 calculations have been performed using the Gaussian package[51]) and with the available experimental estimates. For the H_2O-HCl system the binding energies computed using both MP2 and the BLYP DFT functional are in reasonable agreement with the estimates of HQ methods,[52] and the O−Cl equilibrium distance is close to the experimental estimate. Remarkably, our method is successful also in describing such a "mixed" complex, where a substantial fraction of the binding energy is already reproduced by a standard DFT calculation: in fact, by addition of the VdW corrections to revPBE and BLYP, one obtains binding energies closer to the HQ estimate, while the equilibrium distances, that

TABLE 3: Characteristic Equilibrium Distances, in Å, and Binding Energy, in kcal/mol, of the H_2O-HCl complex, Computed Using Different DFT Functionals, and (in the Case of revPBE and BLYP) Adding the VdW Corrections[a]

method	O−H	O−Cl	E_{bind}
LDA	1.60	2.95	−11.04
PBE	1.83	3.16	−6.41
BLYP	1.88	3.19	−4.89
BLYP + VdW	1.88	3.19	−5.70
revPBE	1.90	3.21	−4.45
revPBE + VdW	1.90	3.21	−5.23
MP2	1.85	3.14	−6.87
HF	2.07	3.34	−4.57
HQ	1.85	3.17	−5.49
exptl		3.22	

[a] Tthe results are compared with calculations performed using MP2, HF, high-quality (HQ) quantum chemistry methods,[52] and the experimental O−Cl estimate.[52]

TABLE 4: O−Cl Equilibrium Distance, in Å, and Binding Energy, in kcal/mol, of the HOH-ClH Complex Computed Using Different DFT Functionals, and (in the Case of revPBE and BLYP) Adding the VdW Corrections[a]

method	O−Cl	E_{bind}
LDA	3.27	−3.87
PBE	3.74	−1.64
BLYP	3.67	−0.81
BLYP + VdW	3.61	−1.34
revPBE	3.82	−0.74
revPBE + VdW	3.77	−1.18
MP2	3.56	−1.68
HF	3.87	−0.92

[a] The results are compared with calculations performed using the MP2 and HF methods.

are already in good agreement with the reference values, are essentially unaffected. Clearly the improvement obtained by summing the VdW corrections to the DFT description is much more dramatic for the weakly bonded HOH-ClH complex (here the MP2 data can be taken as the reference values). In both the H_2O-HCl and HOH-ClH systems, revPBE + VdW and BLYP + VdW give similar results (BLYP + VdW being marginally superior), a behavior which is expected in most of the applications of the method. Interestingly, while LDA clearly overbinds and the HF estimates are similar to those obtained by revPBE, pure PBE performs reasonably well for these specific applications.

C. SiH_4-CH_4. In this particular case, adding the VdW corrections to revPBE appears to still significantly underbind the complex (by comparison with reference literature data, approximately 50% of the actual correlation energy is recovered), so that here the description is much improved if a PBE+VdW scheme is adopted, since pure PBE already gives a significant binding energy. Note that with pure BLYP the system is unbound and with pure revPBE the binding energy is very small and, again, LDA severely overbinds.

For this system we have also investigated the effect of adopting damping functions different from our original choice (eq 11). In particular, we have used the expression proposed by Douketis et al.[10]

$$f_{nl}(r) = [1 - \exp(-2.1r/6 - 0.109r^2/\sqrt{(6)})]^6 \qquad (12)$$

that suggested by Wu and Yang[53]

$$f_{nl}(r) = [1 - \exp(-3.54(r/R_s)^3)]^2 \qquad (13)$$

the one of Tang and Toennies,[54] where the b coefficient is determined by assuming that both the repulsion and the

TABLE 5: Si−C Equilibrium distance, in Å, and Binding Energy, in kcal/mol, of the SiH_4-CH_4 complex, Computed Using Different DFT Functionals, and (in the Case of revPBE and PBE) Adding the VdW Corrections[a]

method	Si−C	E_{bind}
LDA	3.44	−1.89
PBE	4.16	−0.28
PBE + VdW	4.01	−0.83
BLYP	4.07	
revPBE	4.70	−0.05
revPBE + VdW	4.33	−0.37
revPBE + VdW	$(4.18)_1$	$(-0.37)_1$
revPBE + VdW	$(4.18)_2$	$(-0.39)_2$
revPBE + VdW	$(4.18)_3$	$(-0.39)_3$
revPBE + VdW	$(4.18)_4$	$(-0.39)_4$
ref	3.80	−0.81

[a] $(...)_i$ denote results obtained replacing the damping function of eq 11 with that of eq 12 ($i = 1$), eq 13 ($i = 2$), eq 14 ($i = 3$), and eq 15 ($i = 4$). The results are compared with reference literature data.[72]

TABLE 6: Fragment−Fragment Effective C_6 Coefficient (See Text for the Definition), in au, Computed Using the Standard revPBE with the VdW Correction (in Square Parentheses BLYP + VdW), Compared to Available Literature Data[3,10,24,35,73,74] [a]

system	C_6	ref.
benzene dimer S	3010 (2310)	1723 {1311}
benzene dimer PD	2990 (2420)	1723 {1311}
benzene dimer T	3010 (2670)	1723 {1311}
H_2O-HCl	74[77]	77
SiH_4-CH_4	173	209 {199}
Ar−Ar	92.5 (74.7)	64.3 ↔ 65.5
N_2−N_2	90.3 (95.6)	73.4 {67}
CH_4-CH_4	103.0 (101.0)	118.0 ↔ 130.0 {115}
C_6H_6-C_6H_6	2930.0 (2460.0)	1723.0
C_6H_6-Ar	490.0 (448.0)	330.1
CO_2-CO_2	187.0 (172.0)	158.7 {144}
C_6H_6-H_2O	323.0 (299.0)	208.5 ↔ 277.4

[a] We report, in braces, the coefficients computed by Johnson and Becke[72] with a post-HF model; the coefficient for H_2O-HCl has been obtained by using the combination rule and the data reported in ref 24); in parentheses values, computed taking anisotropy effects into account, are reported.

dispersion damping are consequences of wave function overlap

$$f_{nl}(r) = 1 - \exp(-br)\sum_{k=0}^{6}\frac{(br)^k}{k!}$$

$$b = \sqrt{(3)}(1/S_n + 1/S_l) \qquad (14)$$

and, finally, a simple cutoff-function, defined as

$$f_{nl}(r) = 1 \quad \text{for } r \geq R_s$$
$$= 0 \quad \text{for } r < R_s \qquad (15)$$

As can be seen from inspection of Table 5, the effect of adopting different damping functions is very small; in particular it is almost negligible concerning the binding energy, while it is a little more pronounced for the equilibrium distance, due to the fact that the potential energy curves for weakly bonded systems are very shallow. However the same is not true for physisorption on metal surfaces, as reported in the following.

D. Intermolecular C_6 Coefficients. In Table 6, our estimates of the intermolecular C_6 coefficients (including also the values relative to the small molecules already investigated in our previous paper),[14] obtained by averaging over the C_{6nl} MLWFs terms of eq 5, are listed together with the most reliable (to our knowledge) reference corresponding data. As can be seen, for these quantities, the effects of the anisotropy of the MLWFs is much more pronounced: in most of the cases, anisotropic C_6 coefficients are smaller and closer to the reference ones.

Actually, comparison with literature C_6 coefficients should be taken as purely indicative because of different assumed definitions and of difficulties in comparing calculated values and experimental estimates. In fact, usually the C_6 coefficients are derived by fitting experimental data, which actually include also higher-order VdW contributions, so that they "effectively" take into account also the $-C_8/R^8$, $-C_{10}/R^{10}$, etc., terms. Even for noble gas atoms it is not straightforward to compare computed C_6 coefficients with experiment (see, for instance, Harl and Kresse[55]), and the situation clearly becomes worse by increasing the complexity of the systems that are considered (see, for instance, Misquitta and Stone[56]): by inspection of the literature, one can see that the values of effective, intermolecular C_6 coefficients of simple molecules estimated by different ab initio methods are largely scattered; even the MP2 (second order perturbation theory) approach, which is often taken as the benchmark method for testing VdW effects in DFT-corrected schemes, can introduce large errors; for instance, an overestimation of a factor of 2 has been reported for the intermolecular C_6 coefficient of the benzene dimer.[27]

TABLE 7: Ar fcc Crystal: Cohesion Energy per Atom, E_c (meV), Equilibrium Lattice Constant, a (Å), and Bulk Modulus, B_0 (GPa) Computed Using Standard revPBE and PBE Calculations and Adding the VdW Corrections: Results Have Been Obtained Using a Cubic Supercell with 32 Ar Atoms and the Γ Point Sampling of the BZ (Those Reported in Square Parentheses Using Instead a Smaller Cubic Supercell with 4 Ar atoms and a 2 × 2 × 2 BZ Sampling)[a]

method	E_c	a	B_0
LDA	−131 [−133]	4.97 [5.00]	8.4
GGA + SEMI	−118 ↔ −61	5.17 ↔ 6.00	0.9 ↔ 6.0
AIB	−94 ↔ −83	5.20 ↔ 5.30	2.7 ↔ 2.8
revPBE	−7 [−6]	6.70 [6.80]	0.3
revPBE + VdW	−64 [−57]	5.75 [5.85]	1.5
PBE	−22	6.00	0.6
PBE + VdW	−143	5.15	8.2
exptl	−89 ↔ −88	5.23 ↔ 5.30	2.38

method	E_b (Ar_2)	d (Ar_2)
LDA	−30	3.42
revPBE	−2	4.67
revPBE + VdW	−12	4.03
PBE	−6	4.02
expt	−12	3.76

[a] The values are compared to those obtained by LDA, to values obtained by different GGA + VdW semiempirical correction schemes (GGA + SEMI) reported in the literature,[11,55] by ab initio benchmark (AIB) calculations,[75−77] and experiments.[78] For the sake of comparison, we also list the binding energy and equilibrium distance of the Ar dimer (Ar_2), already reported in our previous paper[14] (in an fcc crystal the nearest-neighbor distance is given by $a/\sqrt{2}$).

E. Ar Bulk Crystal. Another sensitive test for our VdW-WF method is represented by the calculation of the cohesion energy of the face-centered cubic (fcc) Ar solid, that is a prototypical crystal with atoms held together only by dispersive forces, where, however, assuming that cohesion is simply given by a sum of 2-body potentials (like the one of the Ar dimer) is incorrect, since interatomic many-body effects are non-

negligible.[57] In Table 7 we compare our results for the minimum-energy lattice constant, the cohesion energy per Ar atom, and the bulk modulus of fcc solid Ar with literature results; we also list the Ar dimer data already reported in our previous paper.[14] To test our approach for a sampling of the BZ not limited to the Γ point, in this case we have performed the calculations both using a cubic supercell with 32 Ar atoms and the Γ-point sampling of the BZ and using a smaller cubic supercell with 4 Ar atoms and a 2 × 2 × 2 BZ sampling. In this system the BLYP functional gives an always repulsive potential curve, pure PBE underbinds, LDA and PBE + VdW clearly overbind (the cohesion energy and the bulk modulus are too large and the lattice constant is too small), while revPBE + VdW gives a reasonable description, although the cohesion energy and the bulk modulus are slightly underestimated and the lattice constant overestimated. Note that values computed using other VdW-corrected schemes are quite scattered, particularly concerning the bulk modulus estimates. In any case, the general behavior of the method found in the Ar crystal resembles that already observed in the Ar dimer.[14]

F. Physisorption on Al Metal Surfaces. We have applied our technique also to the more complex case of Ar, He, and of the saturated H_2 molecule on the Al(100) and Al(111) surfaces. The supercell was orthorhombic with a surface slab made of 32 Al atoms distributed over 4 layers, and a 2 × 2 × 1 sampling of the BZ; no appreciable difference in the equilibrium properties was observed in test calculations with a thicker slab of 64 Al atoms over 8 layers (of course a thicker slab would be instead necessary to describe well the far-from-the-surface, asymptotic behavior, where the binding energy is expected to decay as z^{-3}, z being the fragment-surface distance). Again, electron−ion interactions were described using norm-conserving pseudopotentials (in the case of Al only the 3 valence electrons per atom were explicitly included). In principle, for evaluating adsorption properties in periodically repeated, asymmetric configurations, one should add a dipole correction[58] that compensates for the artificial dipole field introduced by the periodic boundary conditions; however we have checked that, in our cases, this correction is very small (just a few millielectronvolts in the binding energy of Ar on Al(100)).

The physisorption of noble gases on metal and semimetal surfaces has been studied extensively over the years[41,59] because it serves as the paradigm of weak adsorption. Actually, despite the conceived "simplicity" of these systems, even the most basic question (what is the preferred adsorption site?) has not been answered in an entirely satisfactorily way. In principle, because of the nondirectional character of the VdW interactions, sites that maximize the coordination of the adsorbate atom were expected, so that it was typically assumed that the adsorbate occupies the maximally coordinated hollow site. The actual scenario is more complex: for Xe and Kr a clear preference is found[59,60] for adsorption on metallic surfaces in the low-coordination top sites (this behavior was attributed to the delocalization of charge density that increases the repulsive effect at the hollow sites relative to the top site and lifts the potential well upward both in energy and height); for Ar the situation seems to be different: comparison of theoretical and experimental results[59] would suggest that the hollow sites are favored for Ar on Ag(111) and on graphite; although, in this latter case, this configuration is preferred over two other possible sites (top and bridge) by only a few meV.[41]

Physisorption on Al surfaces represents a critical test for our method; in fact the Al case is particularly challenging for a Wannier-based scheme since Al is the metal which most closely approximates a free electron gas system: hence the electronic charge is relatively delocalized and the assumption of exponential localization of the MLWFs is no longer strictly valid.[21] However the following results show that, even in this case, our method works and this does not come to a surprise. In fact, on the one hand, the MLWF technique has been efficiently generalized also to metals;[37,40] on the other, bonding in metallic clusters and in fcc bulk metals (like Al) can be described in terms of H-like orbitals localized on tetrahedral interstitial sites,[40] which is just in line with the spirit of the present scheme.

TABLE 8: Binding Energy, in meV, of Different Physisorbed Systems on Al Surfaces, Computed Using the Standard revPBE Calculation, and Including the VdW Correction, Compared to the LDA Results, and Available Theoretical and Experimental (in Parentheses) Reference Data

system	revPBE	revPBE+VdW	LDA	ref
Ar−Al(100) hollow	−3	−72	−71	
Ar−Al(100) top	−3	−71	−66	
Ar−Al(111) hollow	−3	−77	−89	
Ar−Al(111) top	−3	−79	−92	
H_2−Al(100)	−2	−20	−24	−19[79] (−28[80])
H_2−Al(111)	−2	−22	−61	−19[79] (−37[80])
He−Al(100)	−2	−8	−14	−8,[81] −5[66]
He−Al(111)	−2	−9	−21	−8,[81] −5[66]

TABLE 9: Equilibrium Fragment−Surface Distance, in Å, of Different Physisorbed Systems on Al Surfaces Computed Using the Standard revPBE Calculation and Including the VdW Correction Compared to the LDA Results

system	revPBE	revPBE+VdW	LDA
Ar−Al(100) hollow	5.34	4.66	3.48
Ar−Al(100) top	5.34	4.88	3.57
Ar−Al(111) hollow	5.29	4.95	3.48
Ar−Al(111) top	5.29	5.03	3.46
H_2−Al(100)	5.08	4.62	3.23
H_2−Al(1111	5.16	4.74	3.33
He−Al(100)	4.67	4.45	3.48
He−Al(111)	4.76	4.58	3.89

In the Tables 8 and 9 we report our computed binding energies and equilibrium fragment−surface distances, compared to the most reliable (to our knowledge) experimental and theoretical reference data and to the results of LDA calculations. One has to notice that since the typical spread of the MLWFs is relatively larger in metals than in isolated molecules or insulating systems (like the Ar crystal studied before), the choice of a suitable damping function is here more crucial; by comparison with experimental data available for H_2 and He on Al, we have found that the optimal choice is just given by eq 11. As can be seen, the general performance of the method is quite satisfactory; in fact, the improvement achieved by including the VdW correction, with respect to the pure revPBE scheme (which gives completely unphysical results, namely, a potential well very small and located too far from the surface), is dramatic.

With concern for Ar on Al(100) and Al(111), specific experimental values are not available; however, the experimental binding energy of Ar on several other metals is found to be in the range between 30 and 100 meV[59,61,62] (between 70 and 85 meV for noble metals[63]), in agreement with our VdW-corrected results. We also mention old theoretical estimates of a binding energy of about 200 meV[64] and of 70 meV using a jellium model.[65]

In the case of H_2, the molecule is essentially a free rotor in the physisorption regime,[66] and its interaction with the substrate

exhibits only a slight anisotropy; moreover the effect of changing the position of both He and the H_2 molecule with respect to the substrate is small, so that we report only the results relative to a single, representative configuration. Even for these extremely weakly bonded systems the results are in good agreement with the reference values (we also mention that the binding energy of H_2 on Mg is predicted to be 17 meV[66]). Remarkably, the experimentally observed more favorable binding with the Al(111) surface than with the Al(100) is correctly reproduced by our calculations.

Looking at the tables, one can see that the computed binding energies are reasonable by using the LDA scheme, although this is actually accidental (the well-known LDA overbinding, due to the overestimate of the long-range part of the exchange contribution, somehow mimics the missing VdW interactions); moreover the equilibrium distances are clearly underestimated.

IV. Conclusions

In conclusion, we have presented a detailed description of our recent scheme, developed to include VdW interactions in the DFT by using the MLWFs. We have illustrated the results of successful applications to small molecules, bulk Ar, and the interaction of Ar, He, and H_2 with the Al(100) and Al(111) surfaces. The effects of adopting different damping functions, different reference DFT functionals, and of taking the MLWFs anisotropy into account have been also investigated; moreover, estimates of intermolecular C_6 coefficients have been reported. The good performances of the method clearly indicate that it can be very useful to investigate even relatively complex systems and many realistic surface physics processes, where VdW interactions play a key role. Of a particular value is the possibility of dealing with metal surfaces (insulating surfaces could be somehow treated even using atom-based semiempirical approaches[26]).

Although the present scheme has not been specifically developed for describing weak interactions between isolated molecules but instead for general systems, its validation through applications to the S22 set of Jurečka et al.,[67] consisting of selected, weakly bonded molecular complexes, which has become a standard test set for dispersion including functionals, would allow a better assessment of the performances of the method and is therefore planned for the near future.

Clearly, our method could be further improved in different ways. For instance, by comparing our results with the reference ones, an overestimation of fragment−fragment distances is apparent. Since a similar behavior have been also reported, in a wide range of both finite and extended systems, by Langreth et al.,[8,32] it is likely that it is related to the choice of the revPBE functional (used in typical calculations by Langreth et al. too), and, in particular to the parametrization of the exchange part.[32,68] Hence, more extensive testing of different DFT functionals could be worthwhile.

In the present method the anisotropy of the electron charge distribution is taken into account by considering both the spatial distribution of the MLWFs and the anisotropy of the individual MLWFs. However there could be cases where the symmetry of the relevant localized orbital is clearly qualitatively different from that of s-like, H-like function approximants adopted in the present scheme (for instance when p orbitals are involved); however the generalization of our technique to MLWFs of symmetry different from the s-like one turns out to be straightforward. Moreover, in principle one could adopt gaussians instead of exponential, H-like, functions, because multidimensional integrals are more easily evaluated.[22] For specific applications, partially occupied MLWFs,[25] with improved localization and symmetry properties, could be introduced (this could be of importance particularly for metallic systems): for instance, the benzene molecule, C_6H_6, can be described, (see Figure 1) in terms of localized orbitals, either considering 15 fully occupied states with 6 σ C−H bonds, 3 σ bonds at every second C−C bond, and 3 mixed σ − p double bonds at the 3 remaining C−C bonds, or, alternatively, considering 18 partially occupied states with 6 σ C−H bonds, 6 σ C−C bonds, and 6 half-occupied p orbitals on each C atom. The latter choice would exactly restore the 6-fold rotational symmetry of the benzene molecule.

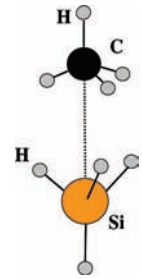

Figure 8. CH_4-SiH_4 molecule.

Finally, a suitable scheme to proper deal with cases where MLWFs belonging to different fragments have a small but non-negligible overlap should be developed, which is relevant particularly for metallic systems.

Acknowledgment. We thank F. Ancilotto, K. Benyahia, M. Boero, S. Grubisič, F. Toigo, and J. Yates for help and useful discussions. We acknowledge allocation of computer resources from INFM "Progetto Calcolo Parallelo" and the support of Padova University through Project CPDA077281-07.

Appendix A: Anisotropy of the MLWFs

To take the anisotropy of the MLWFs into account,[69] if the expressions of eqs 8 and 9 are used, the anisotropic C_{6nl} coefficient, relating the nth WFC, of the first fragment to the lth WFC of the second one, can be defined as

$$C_{6nl} = 1/3C_{6nl}^{\text{ortho}} + 2/3C_{6nl}^{\text{para}} \tag{A1}$$

where

$$C_{6nl}^{\text{ortho}} = \frac{(S_n^{\text{ortho}})^{3/2}(S_l^{\text{ortho}})^3}{2 \cdot 3^{5/4}} F(S_n^{\text{ortho}}, S_l^{\text{ortho}}) \tag{A2}$$

and

$$C_{6nl}^{\text{para}} = \frac{(S_n^{\text{para}})^{3/2}(S_l^{\text{para}})^3}{2 \cdot 3^{5/4}} F(S_n^{\text{para}}, S_l^{\text{para}}) \tag{A3}$$

In the previous equations, S_n^{ortho} and S_n^{para} denote the spreads of the nth MLWF orthogonal and parallel to the nth−lth interfragment distance, R_{nl}, respectively. They can be obtained by considering that

$$R_{nl} = R_{nl}(\alpha, \beta, \gamma), \alpha^2 + \beta^2 + \gamma^2 = 1 \tag{A4}$$

then:

$$\begin{aligned} S_n^{2\text{para}} = \langle r^{\text{para}} r^{\text{para}} \rangle_n = \langle (x\alpha + y\beta + z\gamma)(x\alpha + y\beta + z\gamma) \rangle_n \\ = \alpha^2 \langle x^2 \rangle_n + \beta^2 \langle y^2 \rangle_n + \gamma^2 \langle z^2 \rangle_n + \\ + 2\alpha\beta \langle xy \rangle_n + 2\alpha\gamma \langle xz \rangle_n + 2\beta\gamma \langle yz \rangle_n \end{aligned} \tag{A5}$$

moreover

$$S_n^{2\mathrm{ortho}} = (S_n^2 - S_n^{2\mathrm{para}})/2 \tag{A6}$$

so that

$$S_n^2 = \langle x^2\rangle_n + \langle y^2\rangle_n + \langle z^2\rangle_n = S_n^{2\mathrm{para}} + 2S_n^{2\mathrm{ortho}} \tag{A7}$$

If, for simplicity, we consider a sampling of the BZ limited to the Γ point and a simple cubic supercell of side L (the extension to a general k-point sampling of the BZ and to different supercell symmetries is not difficult), then, in the limit of large L

$$\langle xy\rangle_n \simeq \langle x\rangle_n\langle y\rangle_n + 1/2(L/2\pi)^2(1 - |\langle e^{i2\pi/L(x+y)}\rangle_n|^2) - \\ - 1/2(\langle x^2\rangle_n - \langle x\rangle_n^2) - 1/2(\langle y^2\rangle_n - \langle y\rangle_n^2) \tag{A8}$$

and $\langle x^2\rangle_n$, $\langle x\rangle_n$, $\langle y^2\rangle_n$, and $\langle y\rangle_n$ that are obtained by generating the MLWFs (see eq 2), with similar definitions for $\langle xz\rangle_n$ and $\langle yz\rangle_n$. One can also evaluate the anisotropy, A_{nl}, of the C_{6nl} coefficient as

$$A_{nl} = \frac{2|C_{6nl}^{\mathrm{para}} - C_{6nl}^{\mathrm{ortho}}|}{3C_{6nl}} \tag{A9}$$

Appendix B: Force Estimate

Given a system composed of two fragments, if, for simplicity, the distance between the centers of mass of the fragments is directed along the z axis, then the VdW interfragment force on the second fragment due to to the first one can be easily obtained by assuming that the spreads of the MLWFs do not change appreciably, upon a small displacement of the interfragment distance, so that

$$F_{\mathrm{VdW}} = -\frac{\partial E_{\mathrm{VdW}}}{\partial z} \simeq \sum_{n,l} C_{6nl}\frac{\partial}{\partial z}\left(\frac{f_{nl}(r_{nl})}{r_{nl}^6}\right) \\ = \sum_{n,l} C_{6nl}\frac{\partial}{\partial r_{nl}}\left(\frac{f_{nl}(r_{nl})}{r_{nl}^6}\right)\frac{\partial r_{nl}}{\partial z} \\ = \sum_{n,l} C_{6nl}\frac{\partial}{\partial x}\left(\frac{f_{nl}(x)}{x^6}\right)\frac{\partial r_{nl}}{\partial z} \tag{B1}$$

where

$$\frac{\partial}{\partial x}\left(\frac{f_{nl}(x)}{x^6}\right) = -6/x^7 f(x) + f'^6 \tag{B2}$$

and

$$\frac{\partial r_{nl}}{\partial z} = (z_n - z_l)/r_{nl} \tag{B3}$$

References and Notes

(1) Kohn, W.; Meir, Y.; Makarov, D. E. *Phys. Rev. Lett.* **1998**, *80*, 4153.

(2) Perdew, J. P.; Burke, K.; Ernzerhof, M. *Phys. Rev. Lett.* **1996**, *77*, 3865.

(3) Rapcewicz, K.; Ashcroft, N. W. *Phys. Rev. B* **1991**, *44*, 4032.

(4) Andersson, Y.; Langreth, D. C.; Lundqvist, B. I. *Phys. Rev. Lett.* **1996**, *76*, 102.

(5) Hult, E.; Rydberg, H.; Lundqvist, B. I.; Langreth, D. C. *Phys. Rev. B* **1999**, *59*, 4708.

(6) Dobson, J. F.; Dinte, B. P. *Phys. Rev. Lett.* **1996**, *76*, 1780.

(7) Fuchs, M.; Gonze, X. *Phys. Rev. B* **2002**, *65*, 235109.

(8) (a) Dion, M.; Rydberg, H.; Schröder, E.; Langreth, D. C.; Lundqvist, B. I. *Phys. Rev. Lett.* **2004**, *92*, 246401. (b) Dion, M.; Rydberg, H.; Schröder, E.; Langreth, E.; Lundqvist, B. I. *Phys. Rev. Lett.* **2005**, *95*, 109902. (c) Chakarova-Käck, S. D.; Schröder, E.; Lundqvist, B. I.; Langreth, D. C. *Phys. Rev. Lett.* **2006**, *96*, 146107.

(9) Schwabe, T.; Grimme, S. *Phys. Chem. Chem. Phys.* **2007**, *9*, 3397.

(10) (a) Douketis, C.; Scoles, G.; Marchetti, S.; Zen, M.; Thakkar, A. J. *J. Chem. Phys.* **1982**, *76*, 3057. (b) LeSar, R. *J. Phys. Chem.* **1984**, *88*, 4272. (c) Elstner, M.; Hobza, P.; Frauenheim, T.; Suhai, S.; Kaxiras, E. *J. Chem. Phys.* **2001**, *114*, 5149. (d) Zimmerli, U.; Parrinello, M.; Koumoutsakos, P. *J. Chem. Phys.* **2004**, *120*, 2693.

(11) Ortmann, F.; Bechstedt, F.; Schmidt, W. G. *Phys. Rev. B* **2006**, *73*, 205101.

(12) Wu, X.; Vargas, M. C.; Nayak, S.; Lotrich, V.; Scoles, G. *J. Chem. Phys.* **2001**, *115*, 8748.

(13) Murdachaew, G.; Degironcoli, S.; Scoles, G. *J. Phys. Chem. A* **2008**, *112*, 9993.

(14) Silvestrelli, P. L. *Phys. Rev. Lett.* **2008**, *100*, 053002.

(15) Pisani, C.; Busso, M.; Capecchi, G.; Casassa, S.; Dovesi, R.; Maschio, L.; Zicovich-Wilson, C.; Schütz, M. *J. Chem. Phys.* **2005**, *122*, 094113.

(16) (a) Marzari, N.; Vanderbilt, D. *Phys. Rev. B* **1997**, *56*, 12847. (b) Silvestrelli, P. L.; Marzari, N.; Vanderbilt, D.; Parrinello, M. *Solid State Commun.* **1998**, *107*, 7.

(17) The problem of electronic partitioning, even in large systems such as macromolecules, has been already been addressed; see, for instance Fedorov, D. G.; Kitaura, K. *J. Phys. Chem. A* **2007**, *111*, 6904.

(18) (a) Boys, S. F. *Quantum Theory of Atoms, Molecules, and the Solid State*; Löwdin, P.-O., Ed.; Academic Press, New York, 1966; p 253. (b) Resta, R. *J. Chem. Phys.* **2006**, *124*, 104104.

(19) (a) Vanderbilt, D.; King-Smith, R. D. *Phys. Rev. B* **1993**, *48*, 4442. (b) Resta, R. *Europhys. Lett.* **1993**, *22*, 133.

(20) (a) Wannier90 code by Mostofi, A. A. http://www.wannier.org. (b) WanT code by Ferretti, A. http://www.wannier-transport.org.

(21) (a) Resta, R.; Sorella, S. *Phys. Rev. Lett.* **1999**, *82*, 370. (b) He, L.; Vanderbilt, D. *Phys. Rev. Lett.* **2001**, *86*, 5341. (c) Brouder, C.; Panati, G.; Calandra, M.; Mourougane, C.; Marzari, N. *Phys. Rev. Lett.* **2007**, *98*, 046402.

(22) Slater, J. C. *Quantum Theory of Molecules and Solids*; McGraw-Hill Company, Inc., New York, 1963.

(23) Hirschfelder, J. O.; Löwdin, P. O. *Mol. Phys.* **1959**, *2*, 229.

(24) Halgren, T. A. *J. Am. Chem. Soc.* **1992**, *114*, 7827.

(25) (a) Thygesen, K. S.; Hansen, L. B.; Jacobsen, K. W. *Phys. Rev. Lett.* **2005**, *94*, 026405. (b) Thygesen, K. S.; Hansen, L. B.; Jacobsen, K. W. *Phys. Rev. B* **2005**, *72*, 125119.

(26) Grimme, S.; Antony, J.; Schwabe, T.; Mück-Lichtenfeld, C. *Org. Biomol. Chem.* **2007**, *5*, 741.

(27) Angyan, J. G.; Gerber, I. C.; Savin, A.; Toulouse, J. *Phys. Rev. A* **2005**, *72*, 012510.

(28) (a) Silvestrelli, P. L.; Parrinello, M. *Phys. Rev. Lett.* **1999**, *82*, 3308. (b) Silvestrelli, P. L.; Parrinello, M. *J. Chem. Phys.* **1999**, *111*, 3572.

(29) (a) Car, R.; Parrinello, M. *Phys. Rev. Lett.* **1985**, *55*, 2471. (b) we have used the code CPMD developed by Hutter, H. http://www.cpmd.org/.

(30) Baroni, S.http://www.pwscf.org/.

(31) Zhang, Y.; Yang, W. *Phys. Rev. Lett.* **1998**, *80*, 890.

(32) Thonhauser, T.; Cooper, V. R.; Li, S.; Puzder, A.; Hyldgaard, P.; Langreth, D. C. *Phys. Rev. B* **2007**, *76*, 125112.

(33) (a) Sato, T.; Tsuneda, T.; Hirao, K. *J. Chem. Phys.* **2005**, *123*, 104307. (b) Sato, T.; Tsuneda, T.; Hirao, K. *Mol. Phys.* **2005**, *103*, 1151. (c) Sato, T.; Tsuneda, T.; Hirao, K. *J. Chem. Phys.* **2007**, *126*, 234114. (d) Kamiya, M.; Tsuneda, T.; Hirao, K. *J. Chem. Phys.* **2002**, *117*, 6010.

(34) Tkatchenko, A.; Scheffler, M. *Phys. Rev. Lett.* **2009**, *102*, 073005.

(35) Adamovic, I.; Gordon, M. S. *Mol. Phys.* **2005**, *103*, 379.

(36) Berghold, G.; Mundy, C. J.; Romero, A. H.; Hutter, J.; Parrinello, M. *Phys. Rev. B* **2000**, *61*, 10040.

(37) Iannuzzi, M.; Parrinello, M. *Phys. Rev. B* **2002**, *66*, 155209.

(38) Thomas, J. W.; Iftimie, R.; Tuckerman, M. E. *Phys. Rev. B* **2004**, *69*, 125105.

(39) Iftimie, R.; Thomas, J. W.; Tuckerman, M. E. *J. Chem. Phys.* **2004**, *120*, 2169.

(40) Souza, I.; Marzari, N.; Vanderbilt, D. *Phys. Rev. B* **2001**, *65*, 035109.

(41) Bichoutskaia, E.; Pyper, N. C. *J. Chem. Phys.* **2008**, *128*, 024709.

(42) Grimme, S. *J. Comput. Chem.* **2004**, *25*, 1463.

(43) Walsh, T. R. *Phys. Chem. Chem. Phys.* **2005**, *7*, 443.

(44) Janowski, T.; Pulay, P. *Chem. Phys. Lett.* **2007**, *447*, 27.

(45) Tsuzuki, S.; Honda, K.; Uchimaru, T.; Mikani, M.; Tanabe, K. *J. Am. Chem. Soc.* **2002**, *124*, 104.

(46) Krause, H.; Ernstberger, B.; Neusser, H. J. *Chem. Phys. Lett.* **1991**, *184*, 411.

(47) Grover, J. R.; Walters, E. A.; Hui, E. T. *J. Chem. Phys.* **1987**, *91*, 3233.

(48) Arunan, E.; Gutowsky, H. S. *J. Chem. Phys.* **1993**, *98*, 4294.

(49) (a) Sinnokrot, M. O.; Valeev, E. F.; Sherrill, C. D. *J. Am. Chem. Soc.* **2002**, *124*, 10887. (b) Sinnokrot, M. O.; Sherrill, C. D. *J. Phys. Chem. A* **2004**, *108*, 10200.

(50) Silvestrelli, P. L.; Toigo, F.; Ancilotto, F. *J. Phys. Chem. B* **2006**, *110*, 12022.

(51) Frisch, M. J.; Trucks, G. W.; Schlegel, H. B.; Scuseria, G. E.; Robb, M. A.; Cheeseman, J. R.; Zakrzewski, V. G.; Montgomery, J. A., Jr.; Stratmann, R. E.; Burant, J. C.; Dapprich, S.; Millam, J. M.; Daniels, A. D.; Kudin, K. N.; Strain, M. C.; Farkas, O.; Tomasi, J.; Barone, V.; Cossi, M.; Cammi, R.; Mennucci, B.; Pomelli, C.; Adamo, C.; Clifford, S.; Ochterski, J.; Petersson, G. A.; Ayala, P. Y.; Cui, Q.; Morokuma, K.; Malick, D. K.; Rabuck, A. D.; Raghavachari, K.; Foresman, J. B.; Cioslowski, J.; Ortiz, J. V.; Stefanov, B. B.; Liu, G.; Liashenko, A.; Piskorz, P.; Komaromi, I.; Gomperts, R.; Martin, R. L.; Fox, D. J.; Keith, T.; Al-Laham, M. A.; Peng, C. Y.; Nanayakkara, A.; Gonzalez, C.; Challacombe, M.; Gill, P. M. W.; Johnson, B. G.; Chen, W.; Wong, M. W.; Andres, J. L.; Head-Gordon, M.; Replogle, E. S.; Pople, J. A. *Gaussian 98*, revision A.11.3; Gaussian, Inc.: Pittsburgh, PA, 1998.

(52) Mantz, Y. A.; Geiger, F. M.; Molina, L. T.; Molina, M. J.; Trout, B. L. *J. Phys. Chem. A* **2001**, *105*, 7037.

(53) Wu, Q.; Yang, W. *J. Chem. Phys.* **2002**, *116*, 515.

(54) Tang, K. T.; Toennies, J. P. *J. Chem. Phys.* **1984**, *80*, 3726.

(55) Harl, J.; Kresse, G. *Phys. Rev. B* **2008**, *77*, 045136.

(56) Misquitta, A. J.; Stone, A. J. *Mol. Phys.* **2008**, *106*, 1631.

(57) Tkatchenko, A.; von Lilienfeld, O. A. *Phys. Rev. B* **2008**, *78*, 045116.

(58) Bengtsson, L. *Phys. Rev. B* **1999**, *59*, 12301.

(59) Diehl, R. D.; Seyller, Th.; Caragiu, M.; Leatherman, G. S.; Ferralis, N.; Pussi, K.; Kaukasoina, P.; Lindroos, M. *J. Phys.: Condens. Matter* **2004**, *16*, S2839.

(60) Silva, J. L.; Stampfl, C.; Scheffler, M. *Phys. Rev. Lett.* **2003**, *90*, 066104.

(61) (a) Kirchner, E. J. J.; Kleyn, A. W.; Baerends, E. J. *J. Chem. Phys.* **1994**, *101*, 9155. (b) Kleiman, G. G.; Landman, U. *Solid State Commun.* **1976**, *18*, 819.

(62) Unguris, J.; Bruch, L. W.; Moog, E. R.; Webb, M. B. *Surf. Sci.* **1981**, *109*, 522.

(63) Cheng, E.; Cole, M. W.; Saam, W. F.; Treiner, J. *Phys. Rev. B* **1993**, *48*, 18214.

(64) Andriotis, A. N.; Nicolaides, C. A. *Solid State Commun.* **1984**, *51*, 251.

(65) Lang, N. D. *Phys. Rev. Lett.* **1981**, *46*, 842.

(66) (a) Chizmeshya, A.; Zaremba, E. *Surf. Sci.* **1989**, *220*, 443. (b) Chizmeshya, A.; Cole, M. W.; Zaremba, E. *J. Low Temp. Phys.* **1998**, *110*, 677.

(67) Jurečka, P.; Šponer, J.; Černý, J.; Hozba, P. *Phys. Chem. Chem. Phys.* **2006**, *8*, 1985.

(68) Ziambaras, E.; Kleis, J.; Schröder, E.; Hyldgaard, P. *Phys. Rev. B* **2007**, *76*, 155425.

(69) McLachlan, A. D.; Gregory, R. D.; Ball, M. A. *Mol. Phys.* **1963**, *7*, 119.

(70) Grimme, S. *J. Comput. Chem.* **2006**, *27*, 1787.

(71) Williams, R. W.; Malhotra, D. *Chem. Phys.* **2006**, *327*, 54.

(72) Johnson, E. R.; Becke, A. D. *J. Chem. Phys.* **2005**, *23*, 024101.

(73) Stone, A. J. *The Theory of Intermolecular Forces*; Oxford University Press, Oxford, 1996.

(74) Szczesniak, M. M.; Chalasinski, G.; Cybulski, S. M.; Scheiner, S. *J. Chem. Phys.* **1990**, *93*, 4243.

(75) Lotrich, V. F.; Szalewicz, K. *Phys. Rev. Lett.* **1997**, *79*, 1301.

(76) Rościszewski, K.; Paulus, B.; Fulde, P.; Stoll, H. *Phys. Rev. B* **1999**, *60*, 7905.

(77) Casassa, S.; Halo, M.; Maschio, L. *J. Phys.: Conf. Ser.* **2008**, *117*, 012007.

(78) (a) Tessier, C.; Terlain, A.; Larher, Y. *Physica* **1982**, *113A*, 286. (b) Peterson, O. G.; Batchelder, D. N.; Simmons, R. O. *Phys. Rev.* **1966**, *150*, 703. (c) Schwalbe, L. A.; Crawford, R. K.; Chen, H. H.; Aziz, R. A. *J. Chem. Phys.* **1977**, *66*, 4493. (d) Gewurtz, S.; Stoicheff, P. *Phys. Rev. B* **1974**, *10*, 3487.

(79) Cheng, E. *Phys. Rev. Lett.* **1993**, *70*, 1854.

(80) Andersson, S.; Persson, M.; Harris, J. *Surf. Sci.* **1996**, *360*, L499.

(81) Van Himbergen, J. E.; Silbey, R. *Solid State Commun.* **1977**, *23*, 623.

JP811138N